

Article

# How Fluid Particle Interaction Affects the Flow of Dusty Williamson Fluid

Abdul Rahman Mohd Kasim<sup>1,2,\*</sup>, Nur Syamilah Arifin<sup>3</sup>, Syazwani Mohd Zokri<sup>4,\*</sup> , Noor Amalina Nisa Ariffin<sup>5</sup> and Sharidan Shafie<sup>6</sup> 

<sup>1</sup> Centre for Mathematical Sciences, Universiti Malaysia Pahang, Gambang 26300, Pahang, Malaysia

<sup>2</sup> Center for Research in Advanced Fluid and Process, University Malaysia Pahang, Lebuhraya Tun Razak, Gambang 26300, Pahang, Malaysia

<sup>3</sup> College of Computing, Informatics and Media, Universiti Teknologi MARA, Johor Branch, Pasir Gudang Campus, Masai 81750, Johor, Malaysia

<sup>4</sup> College of Computing, Informatics and Media, Universiti Teknologi MARA, Terengganu Branch, Kuala Terengganu Campus, Kuala Terengganu 21080, Terengganu, Malaysia

<sup>5</sup> College of Computing, Informatics and Media, Universiti Teknologi MARA, Pahang Branch, Jengka Campus, Jengka 26400, Pahang, Malaysia

<sup>6</sup> Department of Mathematical Sciences, Faculty of Science, Universiti Teknologi Malaysia, Johor Bahru 81310, Johor, Malaysia

\* Correspondence: rahmanmohd@ump.edu.my (A.R.M.K.); syazwanimz@uitm.edu.my (S.M.Z.)

**Abstract:** A model of two-phase flow involving non-Newtonian fluid is described to be more reliable to present the fluid that involves industrial applications due to the special characteristics in its behavior. Many models of non-Newtonian fluid were discovered in the last few decades but the model that captured the most attention is the Williamson model. The consideration of the existing particles in the Williamson flow (two-phase Williamson fluid) will make the model more interesting to investigate. Hence, this paper is aimed to explore the flow of two-phase Williamson fluid model in the presence of MHD and thermal radiation circumstances. The obtained ordinary differential equations after the transformations are solved using the Runge-Kutta Fehlberg (RK45) method. The flow is considered asymmetric since it moves over a vertical stretching sheet with external stimuli. The result displays variation in dust phases compared to the fluid phase under distribution of velocity and temperature. It can be concluded that the fluid–particle interaction (FPI) parameter lessening the motion of fluid and heating characteristics. In addition, the upsurges on skin friction and heat transfer are resulting from the rising FPI. Furthermore, the presence of Williamson parameter increases the skin friction while causing degenerations on heat transfer of flow.

**Keywords:** two-phase flow; non-Newtonian fluid; Runge-Kutta Fehlberg (RK45) method



**Citation:** Mohd Kasim, A.R.; Arifin, N.S.; Mohd Zokri, S.; Arifin, N.A.N.; Shafie, S. How Fluid Particle Interaction Affects the Flow of Dusty Williamson Fluid. *Symmetry* **2023**, *15*, 203. <https://doi.org/10.3390/sym15010203>

Academic Editor: Iver H. Brevik

Received: 8 December 2022

Revised: 30 December 2022

Accepted: 5 January 2023

Published: 10 January 2023



**Copyright:** © 2023 by the authors. Licensee MDPI, Basel, Switzerland. This article is an open access article distributed under the terms and conditions of the Creative Commons Attribution (CC BY) license (<https://creativecommons.org/licenses/by/4.0/>).

## 1. Introduction

The fact that it has substantial claims in many engineering glitches such as in petroleum industries, power makers, preservation of nuclear devices, food dispensation and many others, the study of two-phase flow has fascinated the courtesy of many scholars. There are many types of two-phase flow that cover solid–liquid, liquid–liquid, gas–solid, and also the combination of gas–liquid. The combination of the fluid phase and solid phase (particles) in fluid nature is very common since it occurs in many real-life situations. For instance, we may take a look at the case of corpuscle in plasma. The blood and lymph cells can be identified as corpuscle (solid) that suspend in liquid of human body. Besides that, one can see the situation of two-phase flow in boiling flow along the intrusion to the geothermal reservoirs and condensate flow of cold surface in heating pipes and porous insulators. The symmetrical flow can be easily found if the geometry considered is general plate but when it comes to the complex geometry, the flow will be asymmetric.

Since the focus of this research is on the flow features, the important aspects to be considered is the fluid phase type which can be classified as Newtonian and non-Newtonian fluids. Recently, the studies of non-Newtonian fluid have shown robust development. Non-Newtonian fluid differs from the Newtonian fluid in terms of its non-linear connection between stress level and strain due to the dependency of the fluid viscosity deformation. Some studies on Newtonian and non-Newtonian fluid were carried out independently considering the fluid phase only but some focused on both the fluid and solid phase. The available discussion on the particular topic were highlighted by Niknam et al. [1], Han et al. [2], Zokri et al. [3], Khan et al. [4], Basha et al. [5], Kumar et al. [6], Rehman et al. [7] and Ali et al. [8]. The pseudoplastic characteristics were explained by the Williamson model which is significant for a non-Newtonian type of fluid. This model is developed to present the visco-elastic shear thinning fluid at which the viscosity decreases at the improvement of the shear stress rate. Other models which explain quasi-plastic fluids included the Ellis model, the Cross model together with the Carreaus model and the power-law model. However, limited attention was given to the Williamson's flow. Supported by experimental output, the endeavor on the Williamson model started in 1929 by Williamson [9]. Further investigations on this respective model have been continued by many researchers. Khan et al. [10] tackled the suspension of nanoparticles in a Williamson fluid flow over a nonlinear stretching sheet. The investigation on the Williamson fluid moving over a nonlinearly stretching surface embedded with viscous dissipation with the presence of thermal radiation was reported by Megahed [11]. Raza et al. [12] and Salahuddin et al. [13] studied the topics of the Williamson fluid with radiation towards the stretchable geometry and MHD Williamson fluid embedded with exponential viscosity, respectively. Abdal et al. [14] recently discussed the thermal bioconvection dusty Williamson nanofluid caused by an expanding sheet under non-Fourier flux together with radiation circumstance.

However, all the mentioned references are mostly limited to the single-phase flow. The non-Newtonian fluid exploration together with dust particles (two-phase flow) is very scarce and quite interesting to be discovered due to its soundness in presenting the real existing complex fluid in many industrial works. Kasim et al. [15] investigated the fluid and solid interaction of the dusty Casson model over a stretching sheet. The conclusion highlighted the velocity profile which was substantially more affected by the variance in FPI for all the discussed profiles than the temperature profile. Bilal et al. [16] documented the case of Couette flow under viscoelastic with dust particles over a rotating frame. The finding has revealed that the increase in the rotation parameter had caused the retardation in the velocity of dust particles and fluids. The Maxwell's dusty nanofluid embedded with temperature-dependent viscosity together with the influence of solar radiation, surface suction, and changeable surface tension was studied by AlQdah et al. [17]. It was revealed that the strong FPI has improved the Nusselt number. Furthermore, only one former work by Abdal et al. [14] is identified to focus on dusty Williamson nanofluid from an extending sheet. Therefore, the present work aims to contribute to the progress of two-phase Williamson fluid over a vertically stretched sheet in the presence of MHD and thermal radiation effects. The mathematical model is set under a Newtonian heating (NH) state. However, the discussion in this paper is mainly focused on the results when the FPI parameter varies. The solution procedures begin with the transformation of partial differential governing equations (PDEs) into ordinary differential equations (ODEs) to form utilizing similarity variables which are then solved using the Runge-Kutta Fehlberg (RKF45) method.

## 2. Mathematical Formulation

This study aims to reveal the steady flow of a two-dimensional incompressible dusty Williamson fluid over a vertical stretched sheet. It is assumed that the sheet's origin is at the edge of the  $x$ -axis and stretched under  $u_w(x) = ax$ . The Newtonian heating (NH) is applied at the bottom of the plate. The flow has been induced with the align magnetic field for angles ranging from  $0^\circ$  to  $90^\circ$ . Furthermore, the flow was embedded with thermal radiation.

The size of the particle was assumed to be spherical and variations of the particle’s volume fraction as well as buoyancy are ignored with no interacting particles. Figure 1 portrays the flow configuration.

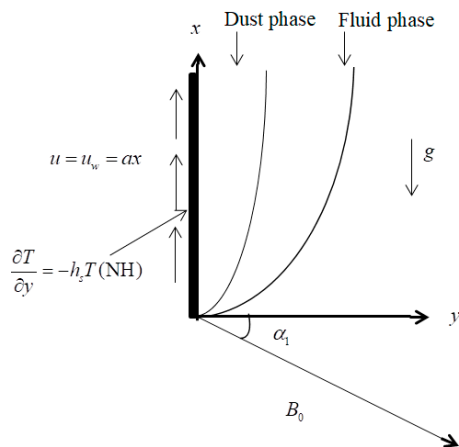


Figure 1. Flow configuration of Dusty Williamson fluid.

The governing equations for the dusty Williamson fluid are described with fluid phase and dust phase. After undergoing Boussinesq and boundary layer approximations, the governing equation are

Fluid phase [18]:

$$\frac{\partial u}{\partial x} + \frac{\partial v}{\partial y} = 0, \tag{1}$$

$$u \frac{\partial u}{\partial x} + v \frac{\partial u}{\partial y} = \nu \frac{\partial^2 u}{\partial y^2} + \sqrt{2\nu}\Gamma \frac{\partial u}{\partial y} \frac{\partial^2 u}{\partial y^2} + \frac{\rho_p}{\rho\tau_v} (u_p - u) - \frac{\sigma u B_0^2}{\rho} \sin^2 \alpha_1, \tag{2}$$

$$u \frac{\partial T}{\partial x} + v \frac{\partial T}{\partial y} = \frac{k}{\rho c_p} \frac{\partial^2 T}{\partial y^2} + \frac{\rho_p c_s}{\tau_T \rho c_p} (T_p - T) - \frac{1}{\rho c_p} \frac{\partial q_r}{\partial y} \tag{3}$$

Dust phase [19]:

$$\frac{\partial}{\partial x} (u_p) + \frac{\partial}{\partial y} (v_p) = 0, \tag{4}$$

$$\rho_p \left( u_p \frac{\partial u_p}{\partial x} + v_p \frac{\partial u_p}{\partial y} \right) = \frac{\rho_p}{\tau_v} (u - u_p), \tag{5}$$

$$\rho_p c_s \left( u_p \frac{\partial T_p}{\partial x} + v_p \frac{\partial T_p}{\partial y} \right) = -\frac{\rho_p c_s}{\gamma_T} (T_p - T) \tag{6}$$

The NH boundary condition are embedded in the model and can be expressed as [20]

$$u = u_w(x) = ax, v = 0, \frac{\partial T}{\partial y} = -h_s T \text{ at } y = 0 \tag{7}$$

$$u \rightarrow 0, u_p \rightarrow 0, v_p \rightarrow v, T \rightarrow T_\infty, T_p \rightarrow T_\infty \text{ at } y \rightarrow \infty$$

Note that, the expression of  $q_r$  which obeys the Rosseland approximation takes the form of [21]

$$q_r = -\frac{4\sigma^*}{3k^*} \frac{\partial T^4}{\partial y} \tag{8}$$

The variables involve in Equations (1)–(8) are summarized as follows:

$(u, v)$	velocities components of the fluid along $x$ and $y$ axes
$(u_p, v_p)$	velocities components of the particle along $x$ and $y$ axes
$\mu$	viscosity of the fluid
$\rho$	density of fluid
$\rho_p$	density of dust
$\alpha_1$	aligned angle
$\tau_v = \frac{1}{k}$	relaxation time of particles phase
$k$	Stoke's resistance (drag force)
$c_p$	specific heat of fluid
$c_s$	specific heat of dust particle
$T$	temperature of fluid
$T_p$	temperature of particle
$\gamma_T$	thermal relaxation time
$q_r$	radiative heat flux
$a$	positive constant
$h_s$	heat transfer parameter
$\sigma^*$	Stefan-Boltzmann constant
$k^*$	Absorption parameter
$T^4$	coefficient linear function of temperature

The Taylor's series is applied to expand  $T^4$  about  $T_\infty$  as

$$T^4 = 4T_\infty^3 T - 3T_\infty^4 \quad (9)$$

In view of Equation (9) into Equation (8), Equation (3) can now be expressed as

$$u \frac{\partial T}{\partial x} + v \frac{\partial T}{\partial y} = k \left( 1 + \frac{16T_\infty^4 \sigma^*}{3kk_1} \right) \frac{\partial^2 T}{\partial y^2} + \frac{\rho_p c_s}{\tau_T \rho c_p} (T_p - T) \quad (10)$$

The similarity transformations that suit the considered model are ([22–24])

$$u = axf'(\eta), v = -(av)^{1/2}f(\eta), \eta = \left(\frac{a}{v}\right)^{1/2}y, \theta(\eta) = \frac{T-T_\infty}{T_\infty} \quad (11)$$

$$u_p = axF'(\eta), v_p = -(av)^{1/2}F(\eta), \theta_p(\eta) = \frac{T_p-T_\infty}{T_\infty},$$

where  $u = \partial\psi/\partial y$  and  $v = -\partial\psi/\partial x$  in which  $\psi$  signifies stream function. Equations (1), (2), (4)–(6) and (10) are now transformed to ordinary differential equations as follow

$$f'''(\eta) + f(\eta)f''(\eta) - (f'(\eta))^2 + \lambda_3 f''(\eta)f'''(\eta) + \beta N(F'(\eta) - f'(\eta)) - M \sin^2 \alpha_1 f'(\eta) = 0, \quad (12)$$

$$\left(1 + \frac{4}{3}R\right)\theta''(\eta) + \text{Pr}f(\eta)\theta'(\eta) + \frac{2}{3}\beta N(\theta_p(\eta) - \theta(\eta)) = 0 \quad (13)$$

$$(F'(\eta))^2 - F(\eta)F''(\eta) + \beta(F'(\eta) - f'(\eta)) = 0, \quad (14)$$

$$\theta_p'(\eta)F(\eta) + \frac{2}{3}\frac{\beta}{\text{Pr}\gamma}(\theta(\eta) - \theta_p(\eta)) = 0 \quad (15)$$

The boundary conditions (7) are changed to

$$f(0) = 0, f'(0) = 1, \theta'(0) = -b(1 + \theta(0)) \text{ at } \eta = 0$$

$$f'(\eta) \rightarrow 0, F(\eta) \rightarrow 0, \theta(\eta) \rightarrow f(\eta), \quad (16)$$

$$\theta(\eta) \rightarrow 0, \theta_p(\eta) \rightarrow 0 \text{ at } \eta \rightarrow \infty$$

The prime ( $\prime$ ) terms are denoted as derivatives to  $\eta$ . The parameters obtained after employing Equation (11) are listed below

$N = \rho_p/\rho$	mass concentration of particle phase
$M = \sigma B_0^2/\rho a$	magnetic field parameter
$\beta = 1/a\tau_v$	fluid-particle interaction
$Pr = \mu c_p/k$	Prandtl number
$\gamma = c_s/c_p$	specific heat ratio of mixture
$b = -h_s(v/a)^{1/2}$	conjugate parameter for NH
$\lambda_3 = \sqrt{2a^3/\nu}\Gamma x$	Williamson parameter
$R = -4\sigma^*T_\infty^3/kk^*$	radiation parameter

The expression of  $C_f$  and  $Nu_x$  are

$$C_f = \frac{\tau_w}{\rho U_\infty^2}, \quad Nu_x = \frac{aq_w}{k(T_w - T_\infty)} \quad (17)$$

where  $\tau_w$  and  $q_w$  are

$$\tau_w = \mu_0 \left[ \frac{\partial u}{\partial y} + \frac{\Gamma}{\sqrt{2}} \left( \frac{\partial u}{\partial y} \right)^2 \right]_{y=0}, \quad q_w = -k \left( \frac{\partial T}{\partial y} \right)_{y=0} \quad (18)$$

Using Equations (17) and (18), the skin friction and Nusselt number coefficient acquired by expressions

$$C_f Re_x^{1/2} = \left( f''(0) + \frac{\lambda_3}{2} (f''(0))^2 \right), \quad Nu_x Re_x^{-1/2} = b \left( 1 + \frac{1}{\theta(0)} \right) \quad (19)$$

### 3. Numerical Procedure and Scope of Investigation

The established method for solving system of ODEs are the Crank–Nicolson method, Runge–Kutta–Fehlberg method, bvp4c, Keller-box method and shooting method. The method of Crank–Nicolson is said to be an unconditionally stable scheme but it involves more computations per time step which results in complexity in finding the solutions. Compared to the RKF45 method, the shooting method, bvp4c and Keller-box method are not self-starting but require the guess of an initial value or condition which led to the instability in generating an output. For that reason, the RKF45 method is implemented in determining the solutions for Equations (12)–(16) by means of its stability, simple to use and acquired self-starting. The computation is conducted by setting the supreme boundary layer thickness for velocity and temperature distribution to be  $\eta_\infty = 6$  with the purpose of satisfying the boundary conditions. The results are visually presented to reveal the flow behavior of two phases characteristics.

The scope of this study is limited to the study on the interaction parameter of a fluid and solid where the focus of parameter  $\beta$  is highlighted.

### 4. Results and Discussion

The characteristics of dusty Williamson fluid correspond to the involved parameters are observed through the plotted graph. Before proceeding with the analysis of this study, a comparative study between the current results and established works needs to be performed to guarantee the authentication of the obtained results. Therefore, the numerical values from the current study for the limiting cases, as in Table 1, are compared with Salleh et al. [23] who tackled the numerical solution of Newtonian fluid without dust particles using the Keller box method and also the exact values by Turkyilmazoglu [25] who analytically solved the micropolar fluid under the absence of the material parameter and wall permeability parameter. It can be noticed that a close agreement between the present results and analytical as well as numerical results is achieved, thus validates the

present numerical algorithm and graphical results. Specifically, the rising Pr values from 3 to 100 has deteriorated the temperature profile.

**Table 1.** Comparative study of  $\theta(0)$  when  $M = \lambda_1 = \beta = N = 0$ ,  $\gamma \rightarrow \infty$  and  $b = 1$ .

Pr	Salleh et al. [23]	Turkyilmazoglu [25]	Present
3	6.02577	6.05158546	6.051585531
5	1.76594	1.76039543	1.760395438
7	1.13511	1.11681524	1.116818808
10	0.76531	0.76452369	0.76452521
100	0.16115	0.14780542	0.147805745

The computation work is then conducted in a way that the values of several parameters such as  $M = 1$ ,  $\alpha_1 = \pi/4$ ,  $\beta = N = 0.5$ ,  $b = 0.3$ ,  $Pr = 10$ ,  $R = 0.2$ ,  $\lambda_1 = 0.1$  and  $\gamma = 0.1$  are kept constants throughout the study unless for the varied parameters. It is worth mentioning the value  $Pr = 10$  was taken from the established document by Basha et al. [5] who established the Falkner–Skan Williamson nanofluid. Since the present study devoted the computational output of the varied values of  $\beta$ ; therefore, only the respective parameter will be discussed graphically.

Figures 2 and 3 display about the variation of  $\beta$  on distribution of velocity and temperature, respectively. The flow of Williamson fluid experiences the deceleration of fluid motion and acceleration of dust particles. This observation can be explained theoretically that as  $\beta$  increases, the relaxation time on dust particles,  $\tau_v$  decreases on account of dust particles are adjusting its velocities to be in the same rate with the motion of fluid. This motivates the dust particles to accelerate until they reach the maximum fluid flow. Consequently, the fluid physically experiences drag forces (Stoke’s Law) when in contact with the dust particles, causing the fluid motion along with its associated momentum boundary layer to retard. A similar trend is observed in the temperature of both phases when  $\beta$  is enlarged from 0.5 to 2.0. The thermal boundary layer is slightly increased due to the incremented  $\beta$  value. It is noticed for both the velocity and temperature profiles, the dust phase showcases a significant graph variation while the fluid phase displays the opposite.

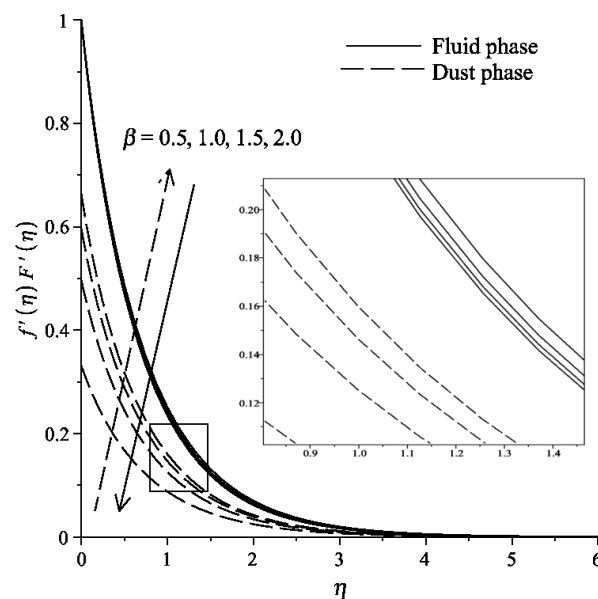


**Figure 2.** Distribution of velocity for variation  $\beta$ .

When the fluid begins to move along the surface, the nearest fluid is dragged, which activates the force coming from friction and counter on flow direction. Along with it, heat starts to move throughout the fluid and surface. When constructing the wall of devices,

these conditions must be taken into consideration as their features can survive high shear stress and temperature. In conjunction with this, the influence of  $\lambda_3$  on  $C_f Re_x^{1/2}$  and  $Nu_x Re_x^{-1/2}$  with different values of  $\beta$  are illustrated in Figures 4 and 5. The respective outputs are very important since the captured behavior can be used to determine the relation in the presence of the fluid and the dust particle. The increasing trend of  $C_f Re_x^{-1/2}$  can be seen as its magnitude value keeps growing as  $\lambda_3$  and  $\beta$  are enhanced. Figure 4 explains the drag-like force generated when the fluid is in contact with dust particles, causing a decrease in the acceleration of the fluid's velocity. Therefore, it can be assumed that the drag force is strengthened by the addition of dust particles, which then enhances the wall shear quantities. The negative sign of  $C_f Re_x^{1/2}$  related to the force on the activities by the surface and fluid. For the physical quantity of  $Nu_x Re_x^{-1/2}$ , as in Figure 5, reveals a decreasing trend in response to the development effect of  $\lambda_3$  for a fixed value of  $\beta$ . Nevertheless, the numerical value appears to rise when  $\beta$  is variously increased for a definite value of  $\lambda_3$ .

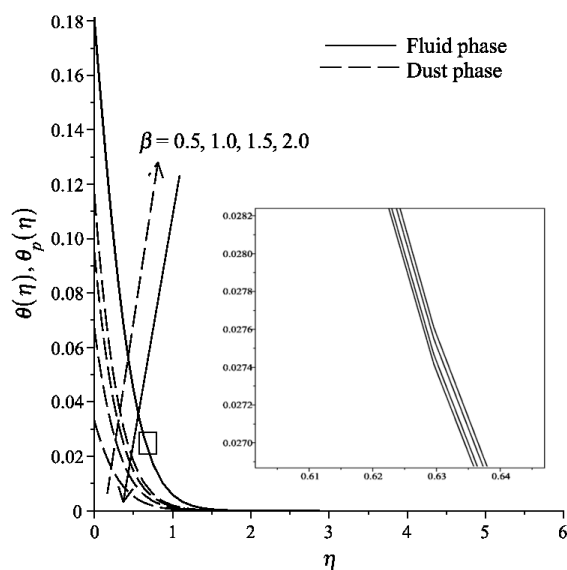


Figure 3. Distribution of temperature for variation  $\beta$ .

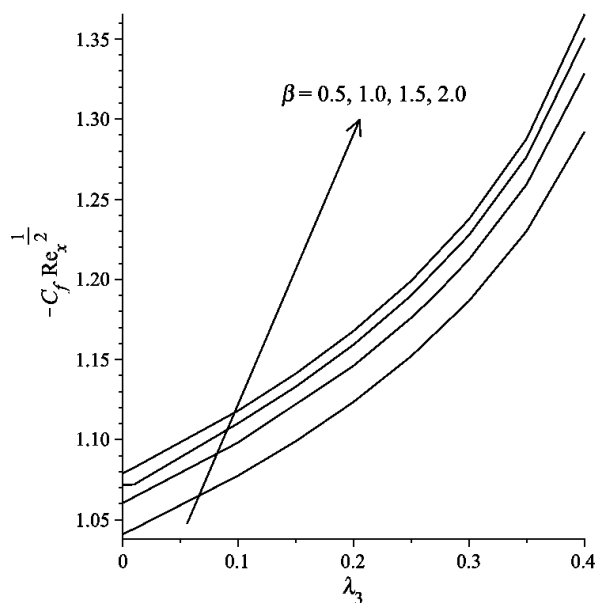
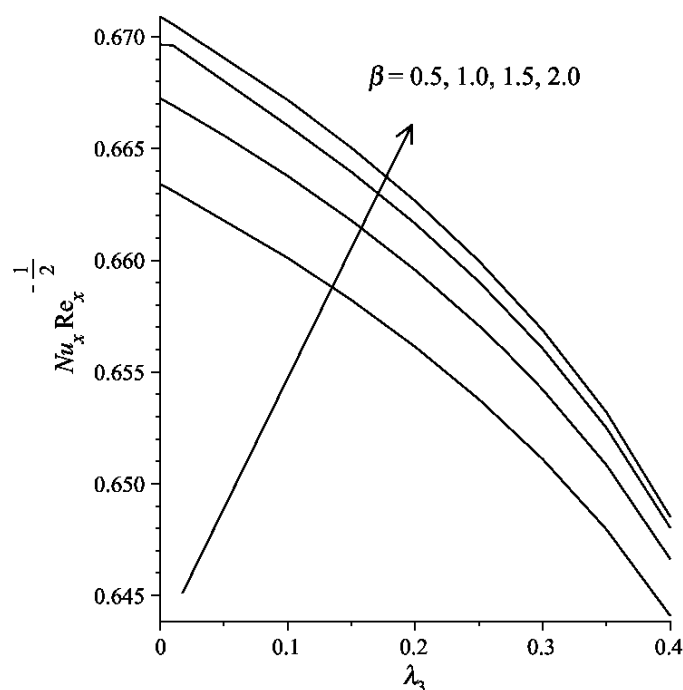


Figure 4. Values of  $\beta$  with  $\lambda_3$  on skin friction quantities.



**Figure 5.** Values of  $\beta$  with  $\lambda_3$  on Nusselt number.

## 5. Conclusions

The flow of the dusty Williamson fluid with thermal radiation and align magnetic accompanied by boundary conditions of NH is analyzed. The mathematical equations of this two-phase flow model are solved by using RKF45 method on the Maple software. It can be concluded that the presence of dust particles affected the Williamson fluid in which its flow propensity changes, as shown in the displayed figures. In addition, this study also delves into the behavior of dust particles in a non-Newtonian fluid. Results obtained here are expected to provide understanding on the two-phase flow from the mathematical point of view. It can be concluded that

- The rising fluid particle interaction has decreased the velocity of fluid phase and increased the velocity of dust phase.
- The incremented fluid particle interaction has increased the temperature of the fluid phase and decreased the temperature of the dust phase.
- The skin friction coefficient has increased due to the fluid–particle interaction and Williamson parameter.
- The heat transfer has increased by reason of the rising fluid–particle interaction and decreased because of the Williamson parameter.

**Author Contributions:** Conceptualization, S.M.Z.; Methodology, N.S.A.; Validation, A.R.M.K. and S.S.; Writing—original draft, A.R.M.K. and N.S.A.; Writing—review and editing, N.A.N.A. All authors have read and agreed to the published version of the manuscript.

**Funding:** This research was funded by Universiti Malaysia Pahang through RDU223015 and Universiti Teknologi MARA (UiTM) through RCF-RACER grant (600-UiTMCTKD (PJI/RMU 5/2/1) RCF-RACER 2021 (7/2021)).

**Data Availability Statement:** Not applicable.

**Acknowledgments:** Thanks to Universiti Malaysia Pahang, Universiti Teknologi MARA Johor Branch, Pasir Gudang Campus, Terengganu Branch, Kuala Terengganu Campus and Pahang Branch, Jengka Campus for the guidance and encouragement. Appreciation also goes to Universiti Teknologi Malaysia.

**Conflicts of Interest:** The authors declare no conflict of interest.

## References

1. Niknam, P.H.; Talluri, L.; Ciappi, L.; Fiaschi, D. Numerical assessment of a two-phase Tesla turbine: Parametric analysis. *Appl. Therm. Eng.* **2021**, *197*, 117364. [[CrossRef](#)]
2. Han, H.; Feng, Y.T.; Owen, D.R.J. Coupled lattice Boltzmann and discrete element modelling of fluid–particle interaction problems. *Comput. Struct.* **2007**, *85*, 11–14. [[CrossRef](#)]
3. Zokri, S.M.; Arifin, N.S.; Mohamed, M.K.A.; Kasim, A.R.M.; Mohammad, N.F.; Salleh, M.Z. Mathematical model of mixed convection boundary layer flow over a horizontal circular cylinder filled in a Jeffrey fluid with viscous dissipation effect. *Sains Malays.* **2018**, *47*, 1607–1615. [[CrossRef](#)]
4. Khan, M.I.; Hayat, T.; Afzal, S.; Khan, M.I.; Alsaedi, A. Theoretical and numerical investigation of Carreau–Yasuda fluid flow subject to Soret and Dufour effects. *Comput. Methods Programs Biomed.* **2020**, *186*, 105145. [[CrossRef](#)] [[PubMed](#)]
5. Basha, H.T.; Sivaraj, R.; Reddy, A.S.; Chamkha, A.J.; Tilioua, M. Impacts of temperature-dependent viscosity and variable Prandtl number on forced convective Falkner–Skan flow of Williamson nanofluid. *SN Appl. Sci.* **2020**, *2*, 477. [[CrossRef](#)]
6. Kumar, R.S.V.; Gowda, R.J.P.; Kumar, R.N.; Radhika, M.; Prasannakumara, B.C. Two-phase flow of dusty fluid with suspended hybrid nanoparticles over a stretching cylinder with modified Fourier heat flux. *SN Appl. Sci.* **2021**, *3*, 384. [[CrossRef](#)]
7. Rehman, S.U.; Fatima, N.; Ali, B.; Imran, M.; Ali, L.; Shah, N.A.; Chung, J.D. The Casson dusty nanofluid: Significance of Darcy–forchheimer law, magnetic field, and non-Fourier heat flux model subject to stretch surface. *Mathematics* **2022**, *10*, 2877. [[CrossRef](#)]
8. Ali, K.; Ahmad, S.; Aamir, M.; Jamshed, W.; Pasha, A.A.; Hussain, S.M. Application of the successive over relaxation method for analyzing the dusty flow over a surface subject to convective boundary condition. *Ain Shams Eng. J.* **2022**, 102044. [[CrossRef](#)]
9. Williamson, R.V. The flow of pseudoplastic materials. *Ind. Eng. Chem.* **1929**, *21*, 1108–1111. [[CrossRef](#)]
10. Khan, M.; Malik, M.Y.; Salahuddin, T.; Hussain, A. Heat and mass transfer of Williamson nanofluid flow yield by an inclined Lorentz force over a nonlinear stretching sheet. *Results Phys.* **2018**, *8*, 862–868. [[CrossRef](#)]
11. Megahed, A.M. Williamson fluid flow due to a nonlinearly stretching sheet with viscous dissipation and thermal radiation. *J. Egypt. Math. Soc.* **2019**, *27*, 12. [[CrossRef](#)]
12. Raza, R.; Mabood, F.; Naz, R.; Abdelsalam, S.I. Thermal transport of radiative Williamson fluid over stretchable curved surface. *Therm. Sci. Eng. Prog.* **2021**, *23*, 100887. [[CrossRef](#)]
13. Salahuddin, T.; Khan, M.; Saeed, T.; Ibrahim, M.; Chu, Y. Induced MHD impact on exponentially varying viscosity of Williamson fluid flow with variable conductivity and diffusivity. *Case Stud. Therm. Eng.* **2021**, *25*, 100895. [[CrossRef](#)]
14. Abdal, S.; Siddique, I.; Din, I.S.U.; Hussain, S. On prescribed thermal distributions of bioconvection Williamson nanofluid transportation due to an extending sheet with non-Fourier flux and radiation. *Waves Random Complex Media* **2022**, 1–20. [[CrossRef](#)]
15. Kasim, A.R.M.; Arifin, N.S.; Zokri, S.M.; Salleh, M.Z.; Mohammad, N.F.; Ching, D.L.C.; Shafie, S.; Ariffin, N.A.N. Convective transport of fluid–Solid interaction: A study between non-Newtonian Casson model with dust particles. *Crystals* **2020**, *10*, 814. [[CrossRef](#)]
16. Bilal, M.; Khan, S.; Ali, F.; Arif, M.; Khan, I.; Nisar, K.S. Couette flow of viscoelastic dusty fluid in a rotating frame along with the heat transfer. *Sci. Rep.* **2021**, *11*, 506. [[CrossRef](#)] [[PubMed](#)]
17. AlQdah, K.S.; Khan, N.M.; Bacha, H.B.; Chung, J.; Shah, N.A. Marangoni convection of dust particles in the boundary layer of Maxwell nanofluids with varying surface tension and viscosity. *Coatings* **2021**, *11*, 1072. [[CrossRef](#)]
18. Nadeem, S.; Hussain, S.T.; Lee, C. Flow of a Williamson fluid over a stretching sheet. *Braz. J. Chem. Eng.* **2013**, *30*, 619–625. [[CrossRef](#)]
19. Siddiq, S.; Hossain, M.A.; Saha, S.C. Two-phase natural convection flow of a dusty fluid. *Int. J. Numer. Methods Heat Fluid Flow* **2015**, *25*, 1542–1556. [[CrossRef](#)]
20. Merkin, J.H.; Nazar, R.; Pop, I. The development of forced convection heat transfer near a forward stagnation point with Newtonian heating. *J. Eng. Math.* **2012**, *74*, 53–60. [[CrossRef](#)]
21. Gireesha, B.J.; Chamkha, A.J.; Manjunatha, S.; Bagewadi, C.S. Mixed convective flow of a dusty fluid over a vertical stretching sheet with non-uniform heat source/sink and radiation. *Int. J. Numer. Methods Heat Fluid Flow* **2013**, *23*, 598–612. [[CrossRef](#)]
22. Ali, F.M.; Nazar, R.; Arifin, N.M.; Pop, I. Mixed convection stagnation-point flow on vertical stretching sheet with external magnetic field. *Appl. Math. Mech.* **2014**, *35*, 155–166. [[CrossRef](#)]
23. Salleh, M.Z.; Nazar, R.; Pop, I. Boundary layer flow and heat transfer over a stretching sheet with Newtonian heating. *J. Taiwan Inst. Chem. Eng.* **2010**, *41*, 651–655. [[CrossRef](#)]
24. Kumar, K.G.; Rudraswamy, N.G.; Gireesha, B.J.; Manjunatha, S. Non linear thermal radiation effect on Williamson fluid with particle-liquid suspension past a stretching surface. *Results Phys.* **2017**, *7*, 3196–3202. [[CrossRef](#)]
25. Turkyilmazoglu, M. Flow of a micropolar fluid due to a porous stretching sheet and heat transfer. *Int. J. Non-Linear Mech.* **2016**, *83*, 59–64. [[CrossRef](#)]

**Disclaimer/Publisher’s Note:** The statements, opinions and data contained in all publications are solely those of the individual author(s) and contributor(s) and not of MDPI and/or the editor(s). MDPI and/or the editor(s) disclaim responsibility for any injury to people or property resulting from any ideas, methods, instructions or products referred to in the content.